

Sustainable chitosan/starch composite material for stabilization of palladium nanoparticles: Synthesis, characterization and investigation of catalytic behaviour of Pd@chitosan/starch nanocomposite in Suzuki–Miyaura reaction

Talat Baran¹  | Nuray Yılmaz Baran²  | Ayfer Mentes¹

¹ Faculty of Science and Letters,
Department of Chemistry, Aksaray
University, 68100 Aksaray, Turkey

² Technical Vocational School,
Department of Chemistry Technology,
Aksaray University, 68100 Aksaray,
Turkey

Correspondence

Talat Baran, Department of Chemistry,
Faculty of Science and Letters, Aksaray
University, 68100 Aksaray, Turkey.
Email: talatbaran_66@hotmail.com

We fabricated a green chitosan/starch composite as support material for stabilization of palladium nanoparticles for the first time. The chemical structure of the sustainable palladium nanocomposite was investigated using various techniques. Characterization studies showed that the average dimensions of the palladium nanocomposite ranged between 16 and 21 nm. The synthesized palladium nanocomposite was employed in the synthesis of a series of biphenyl compounds via Suzuki–Miyaura cross-coupling reactions with an unconventional technique. All coupling reactions were conducted in very short reaction time and excellent biphenyl yields were obtained in the presence of the nanocomposite. The palladium catalyst was tolerant to a wide range of functional groups. We also investigated the recyclability and reusability of the palladium nanocomposite, and found that it could be used for seven successive cycles.

KEYWORDS

chitosan, nanocomposite, reusability, starch

1 | INTRODUCTION

Biopolymers are promising materials as supports for catalytic reactions because of their high thermal stability, high interaction capacity with metal ions and readily enabling chemical modifications.^[1] Additionally, these materials have attracted increasing attention when compared to conventional synthetic supports due to their eco-friendly nature.^[2] Recently, researchers have prepared a variety of catalysts derived from various materials such as chitosan, starch, silica and cellulose, and have studied their activities in catalytic reactions.^[3] However, some bio-based catalysts show lower catalytic activity in reactions due to certain problems as follows: (1) aggregation, (2)

leaching of metal ions and (3) size of particles.^[4] To solve these problems, the synthesis of metallic nanoparticles on solid materials such as silica, zeolite, carbon and graphene has received great attention for catalytic systems because of their easy separation, low cost and low waste.^[5] Among them, carbohydrate polymer composites are regarded as some of the most promising support materials for catalytic systems because of their high surface area and high metal binding capacity.^[6] In the last decade, various metallic nanoparticle catalysts such as silver, gold and platinum on solid materials have been synthesized and their applications have been studied in various fields.^[7] Among these catalysts, palladium nanocatalysts on composites are extraordinarily

important in homogeneous and heterogeneous catalytic systems for increasing the selectivity and reaction yield.^[8] Therefore, palladium nanoparticles stabilized on biopolymers are suitable candidates for Suzuki–Miyaura coupling reactions.

Palladium-catalysed Suzuki–Miyaura coupling reactions represent one of the most important organic synthesis methods, where different unconventional techniques such as microwave and ultrasound irradiations, grinding and photo-activated processes have been applied successfully.^[9] Following a green chemistry approach, environmentally benign Suzuki–Miyaura coupling reactions give a variety of biphenyl compounds which are widely used in cosmetics, pharmacology, drug discovery, agricultural compounds, etc.^[10] Suzuki–Miyaura reactions have high tolerance for various functional groups when compared to other cross-coupling reactions.^[11] Therefore, researchers have made continuing efforts to develop new homogeneous and heterogeneous catalysts or catalyst systems for Suzuki–Miyaura reactions since the discovery of these reactions.^[12] Considering excellent catalytic activity and selectivity, researchers have showed greater interest in heterogeneous catalysts than homogeneous ones for Suzuki–Miyaura coupling reactions.^[13]

In the study reported here, (1) we produced a new chitosan/starch (CS/ST) composite as support material for palladium nanoparticles and its structure was investigated using various analytical tools, (2) a Pd@chitosan/starch nanocomposite was designed using the CS/ST composite and (3) the catalytic behaviour of the Pd@chitosan/starch nanocomposite was investigated in Suzuki–Miyaura cross-coupling reactions using the direct interaction of electromagnetic irradiation with molecules in the reaction mixture with very short reaction times under solvent-free conditions. Characterization studies showed CS/ST and Pd@chitosan/starch nanocomposite were successfully prepared. We found that the novel palladium nanocomposite showed excellent catalytic performance towards the coupling reactions of phenylboronic acid with a series of aryl halides, and desired biphenyl products were produced in yields of up to 99%. Moreover, reusability investigation revealed that the palladium nanocomposite was easily recovered from reaction media and showed superior stability for several successive cycles without significant loss of its activity.

2 | EXPERIMENTAL

2.1 | Materials

Chitosan, starch, Na₂PdCl₄, KOH, NaHCO₃, NaOH, Cs₂CO₃, K₂CO₃, MgSO₄, NaBH₄, phenylboronic acid, aryl

halides, toluene, ethanol and acetic acid were purchased from Sigma-Aldrich.

2.2 | Instrumentation

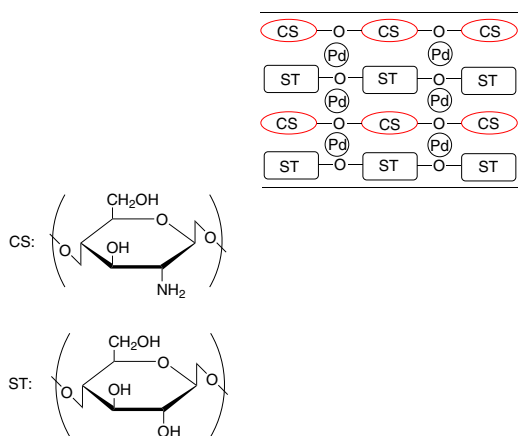
Fourier transform infrared (FT-IR) spectra of CS/ST and Pd@chitosan/starch nanocomposite were obtained with a PerkinElmer Spectrum 100 FT-IR spectrophotometer. X-ray diffraction (XRD) patterns were recorded using a Rigaku Smart Lab system (at 40 kV, 30 mA; and 2θ scan angle of 10–70°). Thermal and mechanical durability of CS/ST and Pd@chitosan/starch nanocomposite were studied with an EXSTAR S11 7300 (nitrogen atmosphere; 30–650 °C heating range). The surface properties of samples were determined using scanning electron microscopy (SEM) with a QUANTA-FEG 250 ESEM by coating samples with platinum. The analysis of Pd ions on CS/ST was conducted using energy-dispersive X-ray (EDX) analysis with an EDAX-Metek. Palladium ion content of the Pd nanocomposite was determined using a PerkinElmer Optima 2100 DV inductively coupled plasma (ICP) optical emission spectrometer (OES). GC–MS analysis of biphenyl compounds was performed with an Agilent GC-7890A-MS 5975. ¹H NMR spectra of biphenyl compounds were recorded with an Agilent 600 MHz spectrometer using acetone-d₆ as solvent. A domestic microwave oven was used in the catalytic tests.

2.3 | Production of palladium nanoparticles on CS/ST

Chitosan (1 g) was dissolved in a solution of 2% acetic acid (100 ml). Starch (1 g) was added to the reaction media, which was stirred overnight at room temperature to obtain the CS/ST composite. Then, 0.2 g of Na₂PdCl₄ in 10 ml of water was added dropwise to the reaction mixture and stirred for 3 h. Subsequently, freshly prepared NaBH₄ solution (0.8 M, 10 ml in water) was added to the reaction media to reduce Pd(II) to Pd(0) and we immediately observed that the light yellow colour of the solution turned dark grey. The resulting mixture was stirred for 30 min. Finally, the pH of the reaction solution was adjusted to neutral pH with NaOH solution, and the Pd@chitosan/starch nanocomposite was filtered and washed with distilled water and allowed to dry at room temperature (Scheme 1).

2.4 | Optimal conditions for Suzuki–Miyaura coupling reactions

To find the optimal reaction conditions for Suzuki–Miyaura reactions, we investigated the effect of parameters such as base, catalyst loading and reaction time on

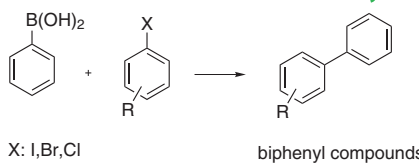


SCHEME 1 Synthesis pathway of Pd@chitosan/starch nanocomposite

the yield of 4-methoxybiphenyl which was synthesized from the coupling reaction of phenylboronic acid with 4-bromoanisole as model reaction. The model coupling reaction was performed with various inorganic bases such as NaOH, KOH, NaHCO₃, Cs₂CO₃ and K₂CO₃ to determine the most suitable base system. We observed that NaOH, KOH and NaHCO₃ did not have a significant influence on the biphenyl yields (17, 28 and 15%, respectively). On the other hand, a moderately high reaction yield was obtained with Cs₂CO₃ (80%). Among the bases, K₂CO₃ gave the highest reaction yield (98%) and so we decided to use K₂CO₃ as base system. The model coupling reaction was carried out within 1–6 min to determine the optimal time and we recorded a linear increase in the reaction yield up to 5 min (1 min, 20% yield; 2 min, 35% yield; 3 min, 68% yield; 4 min, 79% yield; 5 min, 88% yield; 6 min, 98% yield). However, biphenyl yield did not change for longer reaction time (7 min, 98% yield), and so, based on these experimental findings, we opted for 6 min as the optimal reaction time. We also attempted to find an optimal catalyst loading for the Suzuki–Miyaura reaction and we conducted preliminary studies with various amounts of catalyst. The optimum catalyst loading was determined as 0.005 mol% (0.001 mol% catalyst, 25% yield; 0.002 mol% catalyst, 58% yield; 0.003 mol% catalyst, 80% yield; 0.004 mol% catalyst, 88% yield; 0.005 mol% catalyst, 98% yield; 0.006 mol% catalyst, 98% yield).

2.5 | General procedure for Suzuki–Miyaura coupling reactions

A typical cross-coupling reaction was carried out as follows (Scheme 2). A mixture of aryl halide (1.12 mmol), phenylboronic acid (1.87 mmol), potassium carbonate (3.75 mmol) and Pd@chitosan/starch nanocomposite (0.005 mol%) was added to a Schlenk tube and the resulting heterogeneous mixture was exposed to 400 W



SCHEME 2 General synthesis scheme of Suzuki–Miyaura reactions

microwave irradiation for 6 min at 50 °C. After completion of the coupling reaction, the reaction mixture was cooled to room temperature. Then the solid palladium nanocomposite was separated by filtration. A mixture of toluene (4 ml) and water (2 ml) was added to the reaction solution and extracted three times. Finally, the organic phase containing the desired biphenyl compounds was subjected to GC–MS for characterization. Turnover number (TON) and turnover frequency (TOF; as mol product (mol catalyst)⁻¹ h⁻¹) of all coupling reactions were calculated.^[14]

3 | RESULTS AND DISCUSSION

3.1 | Characterization of nanocomposite

3.1.1 | FT-IR analysis

Figure 1 shows the FT-IR spectra of CS/ST and Pd@chitosan/starch nanocomposite. When the FT-IR spectrum of CS/ST was examined, we observed important bands belonging to chitosan and starch. These include: 3294 cm⁻¹ (—OH stretching of starch), 2930 cm⁻¹ (—C—H stretching of starch), 1644 cm⁻¹ (—C—O stretching of chitosan), 1563 cm⁻¹ (NH₂ bending of chitosan), 1150 cm⁻¹ (C—O—C stretching of chitosan and starch) and 1015 cm⁻¹ (C—O stretching chitosan and starch).^[15, 3b] The presence of these peaks in the spectrum showed that CS/ST was successfully formulated. We observed that the FT-IR spectrum of Pd@chitosan/starch nanocomposite was similar to that of CS/ST. However, peak intensities of Pd@chitosan/starch nanocomposite decreased and the peaks shifted to lower wavenumbers compared to CS/ST. These important changes can be attributed to bonding interactions between the functional groups of CS/ST and palladium ions.^[16]

3.1.2 | SEM/EDX analysis

Surface morphology and microstructure of CS/ST and Pd@chitosan/starch nanocomposite were explored using SEM analysis and the micrographs are shown in Figure 2. From the SEM image, we observed that CS/ST had coarse irregular morphology characteristics

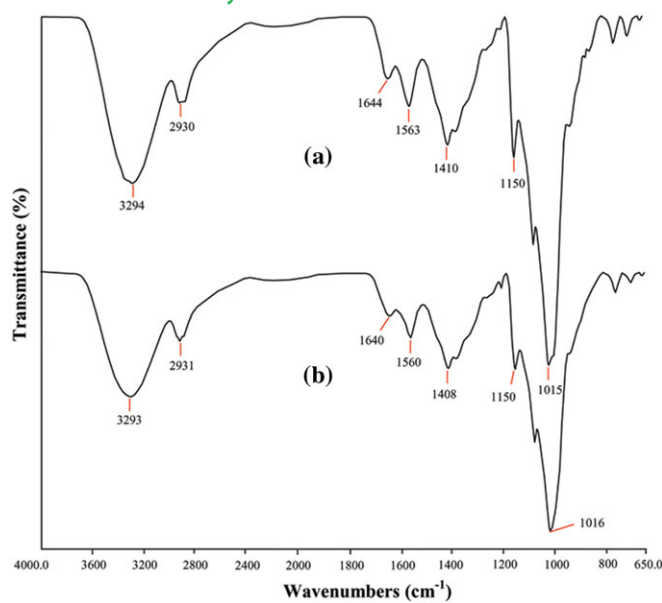


FIGURE 1 FT-IR spectra of (a) CS/CT and (b) Pd@chitosan/starch nanocomposite

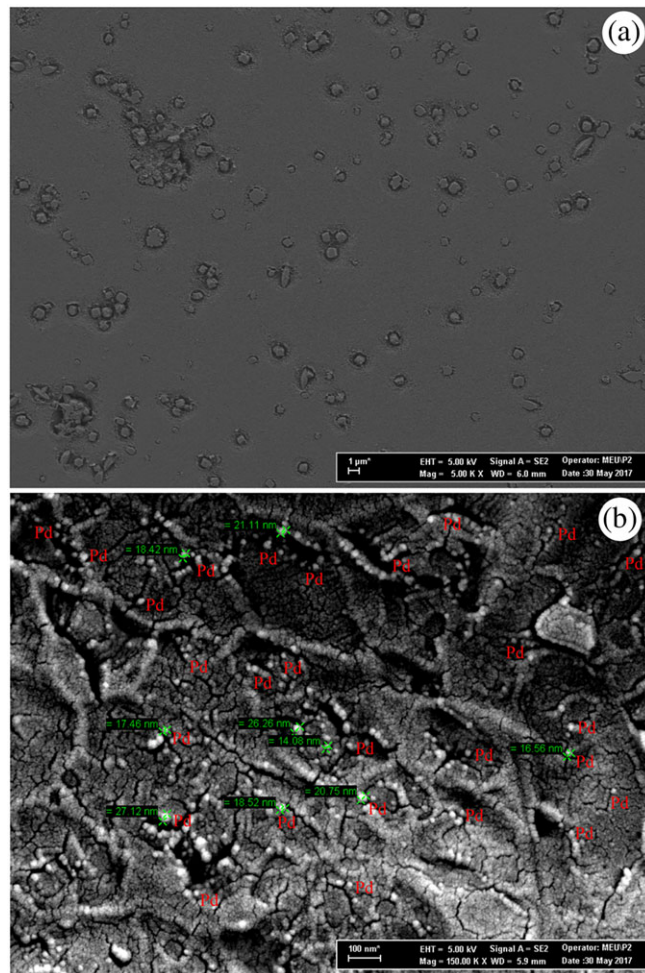


FIGURE 2 SEM images of (a) CS/CT and (b) Pd@chitosan/starch nanocomposite

(Figure 2a). As seen from Figure 2(b), the Pd@chitosan/starch nanocomposite had a spherical morphology structure. The average diameters of Pd@chitosan/starch

nanocomposite particles were found to be between 16 and 21 nm. It is noteworthy that palladium ions were homogeneously distributed on the CS/ST surface and no

aggregation formation was observed in the micrograph of the Pd@chitosan/starch nanocomposite. To confirm the presence of palladium ions on the CS/ST matrix, we conducted EDX analysis of the Pd nanocomposite (Figure 3). The signal of Pd was clearly displayed in the EDX spectrum. This signal revealed that Pd@chitosan/starch nanocomposite was formed on the composite matrix. In addition, Pd content on the CS/ST matrix was analysed using both ICP-OES and EDAX and found as 2.61 and 2.53%, respectively. These very close values revealed that Pd nanoparticles were homogeneously dispersed on the CS/ST surface.

3.1.3 | XRD analysis

To evaluate the structure of CS/ST and Pd@chitosan/starch nanocomposite, XRD analysis was carried out and the patterns are shown in Figure 4. We observed two strong and sharp peaks at 9.3° and 20.4° in the spectrum of CS/ST (Figure 4a). These peaks can be attributed to saccharide peaks of chitosan and starch, respectively.^[15, 3b] In

the pattern of Pd@chitosan/starch nanocomposite (Figure 4b), three characteristic peaks are observed at 40° , 46° and 68° which correspond to crystallographic planes of Pd(0).^[17] These peaks show that Pd(II) was successfully reduced to Pd(0).

3.1.4 | Thermogravimetric (TG)/differential TG (DTG) analysis

TG/DTG analyses of CS/ST and Pd@chitosan/starch nanocomposite were carried out to determine the thermal stability of samples. The obtained curves are shown in Figure 5. From Figure 5(a), maximum thermal decay of CS/ST was found at $217.3\text{ }^\circ\text{C}$. In addition, we observed four main degradation stages for CS/ST. The first degradation stage (6.09%) corresponds to the adsorbed water on the composite. In the second major degradation step, 22.15% loss of mass can be related to degradation of chitosan saccharide rings. The third step of 20.42% mass loss can be due to degradation of starch saccharide rings. The closeness of mass losses of these degradation steps

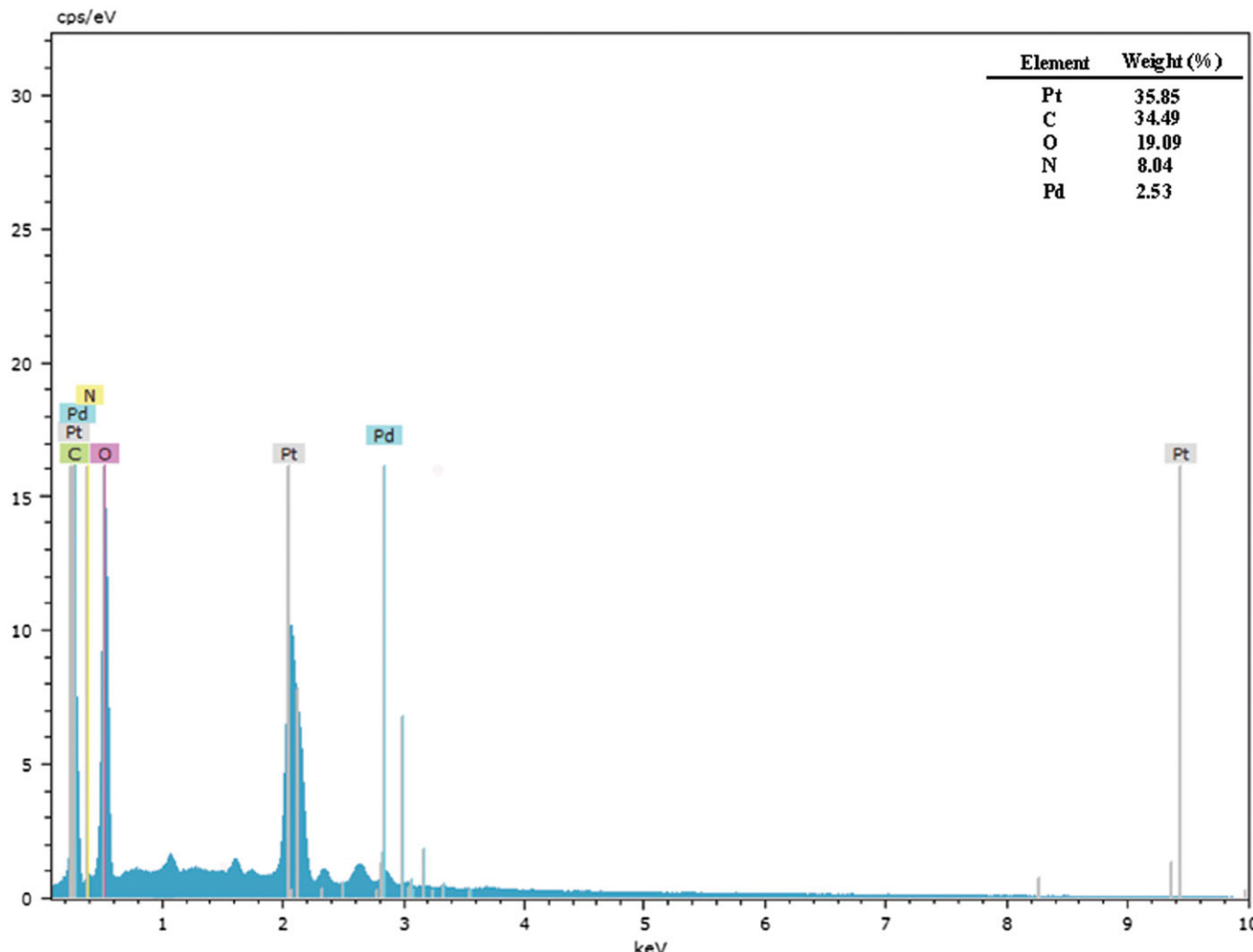


FIGURE 3 EDX spectrum of Pd@chitosan/starch nanocomposite

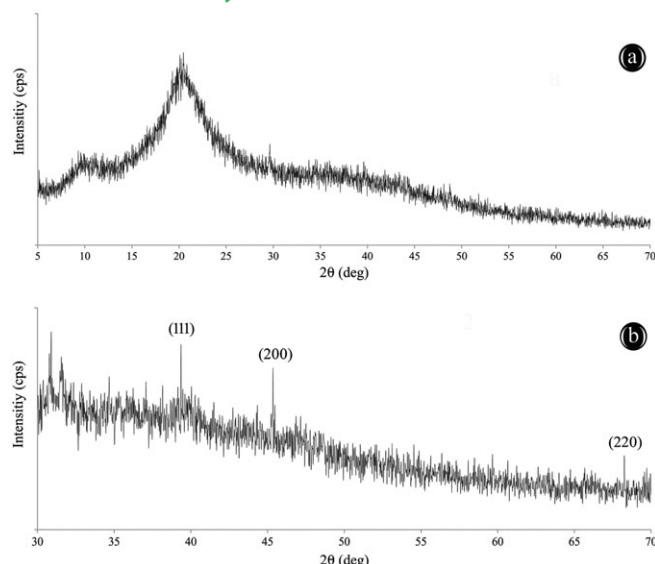


FIGURE 4 XRD patterns of (a) CS/CT and (b) Pd@chitosan/starch nanocomposite

can be explained by the fact that the composition of the composite is nearly 1:1. The last degradation step can be attributed to the thermal decay of the glucosamine residuals of chitosan and starch. We observed a slightly higher degradation temperature for Pd@chitosan/starch nanocomposite (263.3 °C), indicating that it is suitable for catalytic reactions (Figure 5b). This difference of thermal stabilities between composite and catalyst provides important evidence for the formation of palladium nanocatalyst on CS/ST.

3.2 | Catalytic behaviour of palladium nanocomposite in Suzuki reactions

Using the optimized conditions mentioned in Section 1.4, we examined the catalytic performance of the palladium nanocomposite in the synthesis of 23 different biphenyl compounds via Suzuki–Miyaura coupling reactions. The results are summarized in Table 1. Excellent biphenyl product yields were obtained with aryl iodides (entries 11–16). The coupling reaction of the aryl iodide with *para*—OCH₃ group produced excellent biphenyl yield of 99%. Aryl iodide bearing electron-withdrawing —NO₂ group at the *meta* position gave excellent reaction yield of 90%. The 4-NH₂ aryl iodide also gave good biphenyl yield (88%). Electron-withdrawing group —CH₃ at *ortho*, *meta* and *para* positions of aryl iodides gave good reaction yields of 55, 70 and 75%, respectively (entries 14–16). Also, we observed that the cross-coupling reactions of aryl bromides with phenylboronic acid provided excellent biphenyl yields (entries 1–10). For example, high reaction yields were reached with aryl bromides containing —OCH₃ at the *ortho*, *meta* and *para* position: 82, 87 and 98%, respectively. Excellent biphenyl yields of 80 and 95% were reached with the coupling reactions of *meta*-

or *para*-bromonitrobenzene and phenylboronic acid. Outstanding product yield was also obtained with aryl bromide containing electron-withdrawing group —CN (90%). Aryl bromides with *meta*- and *para*-substituted —NH₂ gave good product yields of 72 and 83%. However, moderately high reaction yields of 55 and 72% were obtained with aryl bromides which contain electron-donating *ortho*- and *para*-substituted —CH₃ group, respectively. We also tested the effectiveness of the palladium nanocomposite in the reactions of aryl chlorides which generally have poor reactivity in Suzuki–Miyaura reactions and obtained good reaction yields (entries 17–23).^[18] For example, the Pd nanocomposite produced good results in the presence of electron-withdrawing —NO₂ and —CN substituent groups on aryl chlorides: 73 and 75% yields, respectively. Additionally, we also obtained good product yields with *ortho*, *meta* and *para* —OCH₃ group on the substrate (48, 60, 70%, respectively). On the other hand, the lowest product yields were reached with aryl chlorides having *ortho*, *meta* and *para* —CH₃ group which shows electron-donating characteristics. Taking into account the obtained results, the novel palladium nanocomposite showed excellent catalytic behaviour in Suzuki–Miyaura cross-coupling reactions. These findings reveal that the palladium catalyst is tolerant to a wide range of functional groups in Suzuki–Miyaura cross-coupling reactions.

TON and TOF values of any catalyst play a crucial role in its industrial applicability. So, we calculated the TON and TOF values for all coupling reactions and the findings are presented in Table 1. High TONs (19 800) and TOFs (198 000) were reached using very small amount of Pd@chitosan/starch nanocomposite. These findings showed the catalyst can be used in different industrial applications due to the high TONs TOFs. In addition,

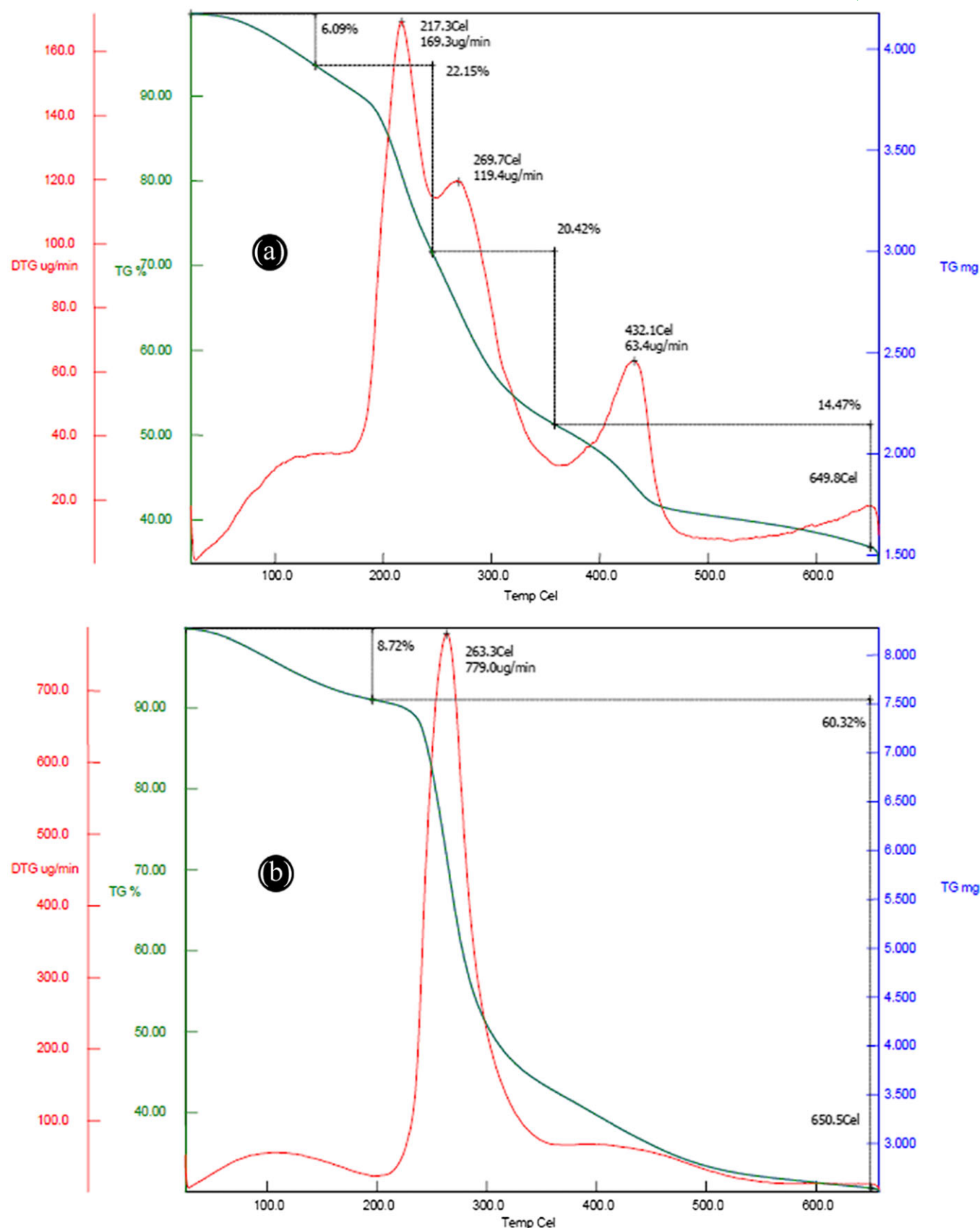


FIGURE 5 TG/DTG curves of (a) CS/CT and (b) Pd@chitosan/starch nanocomposite

TABLE 1 Suzuki–Miyaura reactions of aryl halides and phenylboronic acid in the presence of Pd@chitosan/starch nanocomposite^a

Entry	Phenylboronic acid	Aryl halide	Product	Biphenyl yield (%)	TON	TOF
1	<chem>c1ccccc1B(O)2</chem>	<chem>Br-c1ccccc1OCH3</chem>	<chem>c1ccccc1-c2ccccc2OCH3</chem>	98	19 600	196 000
2	<chem>c1ccccc1B(O)2</chem>	<chem>Br-c1ccccc1OCH3</chem>	<chem>c1ccccc1-c2ccccc2OCH3</chem>	87	17 400	174 000
3	<chem>c1ccccc1B(O)2</chem>	<chem>Br-c1ccccc1C(=O)O</chem>	<chem>c1ccccc1-c2ccccc2C(=O)O</chem>	82	16 400	164 000
4	<chem>c1ccccc1B(O)2</chem>	<chem>Br-c1ccccc1N</chem>	<chem>c1ccccc1-c2ccccc2N</chem>	83	16 600	166 000
5	<chem>c1ccccc1B(O)2</chem>	<chem>Br-c1ccccc1N</chem>	<chem>c1ccccc1-c2ccccc2N</chem>	72	14 400	144 000
6	<chem>c1ccccc1B(O)2</chem>	<chem>Br-c1ccccc1C#N</chem>	<chem>c1ccccc1-c2ccccc2C#N</chem>	90	18 000	180 000
7	<chem>c1ccccc1B(O)2</chem>	<chem>Br-c1ccccc1N#O2</chem>	<chem>c1ccccc1-c2ccccc2N#O2</chem>	95	19 000	190 000
8	<chem>c1ccccc1B(O)2</chem>	<chem>Br-c1ccccc1N#O2</chem>	<chem>c1ccccc1-c2ccccc2N#O2</chem>	80	16 000	160 000
9	<chem>c1ccccc1B(O)2</chem>	<chem>Br-c1ccccc1C#</chem>	<chem>c1ccccc1-c2ccccc2C#</chem>	72	14 400	144 000
10	<chem>c1ccccc1B(O)2</chem>	<chem>Br-c1ccccc1C</chem>	<chem>c1ccccc1-c2ccccc2C</chem>	55	11 000	110 000
11	<chem>c1ccccc1B(O)2</chem>	<chem>I-c1ccccc1OCH3</chem>	<chem>c1ccccc1-c2ccccc2OCH3</chem>	99	19 800	198 000
12	<chem>c1ccccc1B(O)2</chem>	<chem>I-c1ccccc1N</chem>	<chem>c1ccccc1-c2ccccc2N</chem>	88	17 600	176 000
13	<chem>c1ccccc1B(O)2</chem>	<chem>I-c1ccccc1N#O2</chem>	<chem>c1ccccc1-c2ccccc2N#O2</chem>	90	18 000	180 000
14	<chem>c1ccccc1B(O)2</chem>	<chem>I-c1ccccc1C#</chem>	<chem>c1ccccc1-c2ccccc2C#</chem>	75	15 000	150 000
15	<chem>c1ccccc1B(O)2</chem>	<chem>I-c1ccccc1C</chem>	<chem>c1ccccc1-c2ccccc2C</chem>	70	14 000	140 000
16	<chem>c1ccccc1B(O)2</chem>	<chem>I-c1ccccc1C(=O)C</chem>	<chem>c1ccccc1-c2ccccc2C(=O)C</chem>	55	11 000	111 000

(Continues)

TABLE 1 (Continued)

Entry	Phenylboronic acid	Aryl halide	Product	Biphenyl yield (%)	TON	TOF
17				70	14 000	140 000
18				60	12 000	120 000
19				48	9 600	96 000
20				75	15 000	150 000
21				73	14 600	146 000
22				45	9 000	90 000
23				35	7 000	70 000

^aReaction conditions: 1.12 mmol aryl halide, 1.87 mmol phenylboronic acid, 3.75 mmol K₂CO₃, 0.005 mol% Pd@chitosan/starch nanocomposite, 50 °C, 0.1 h, microwave irradiation.

TABLE 2 Comparison of catalytic performance of Pd@chitosan/starch nanocomposite with that of other catalysts in Suzuki cross-coupling reactions

Catalyst	Yield (%)	Time	Temperature (°C)	Ref.
Fe ₃ O ₄ @CS-Schiff base Pd catalyst	97	20 min	80	[19]
CS-g-mPEG350 Pd(0) catalyst	92	0.33 h	150	[1]
Pd-NPs@chitosan	96	5 h	70	[20]
Chitosan-supported palladium(0) catalyst	95	15 min	150	[2]
CMC-NHC-Pd	96	3 h	60	[3c]
Cell-Pd(0)	96	5.5 h	100	[21]
Nano-Pd	97	30 min	80	[22]
Pd@chitosan/starch nanocomposite	99	6 min	50	Present study

we compared the catalytic activity of Pd@chitosan/starch nanocomposite with that of other catalysts reported in the literature (Table 2). In terms of high reaction yields obtained in very short reaction times, very low catalyst loading and tolerance to a broad range of functional groups on the substrate, Pd@chitosan/starch nanocomposite is advantageous compared to the other catalysts.

In addition, characterization of obtained biphenyl compounds was performed using GC-MS and ¹H NMR analysis. The results are given in the supporting information.

3.3 | Reusability of Pd@chitosan/starch nanocomposite

From the viewpoint of industrial usability, a major property for any catalyst is its ability to be recycled.^[3b] Therefore, we decided to investigate the sustainability of Pd@chitosan/starch nanocomposite on the model coupling reaction under determined optimal conditions. After the first recycling test, the catalyst was filtered and rinsed with hot methanol and water for subsequent

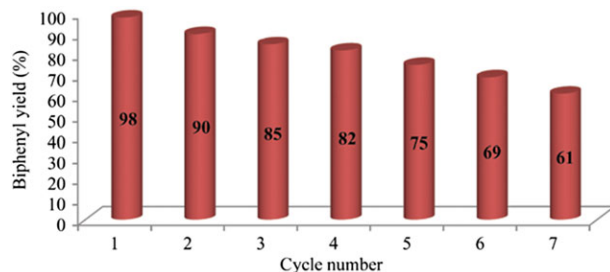


FIGURE 6 Reusability of Pd@chitosan/starch nanocomposite

runs. This regeneration process was repeated at end of the each cycle and the same Pd@chitosan/starch nanocomposite was used in the reactions. Reusability tests revealed that Pd@chitosan/starch nanocomposite could be recycled for seven successive runs (Figure 6). This unique property shows that Pd@chitosan/starch nanocomposite can be used in various industrial applications. Additionally, we performed FT-IR analysis of the catalyst after the reusability tests to determine the changes in the chemical structure of the catalyst. We did not observe any significant change of the FT-IR spectrum of the catalyst compared to that of fresh catalyst. This analysis showed that the Pd@chitosan/starch nanocomposite preserved its chemical structure after the successive reaction runs.

4 | CONCLUSIONS

In summary, a sustainable Pd@chitosan/starch nanocomposite was synthesized for the first time, and its chemical characterization was carried out using FT-IR, TG/DTG, SEM/EDX, XRD and ICP-OES analytic tools. Spectroscopic studies showed that Pd@chitosan/starch nanocomposite was immobilized successfully on the CS/CT surface and the average size of Pd@chitosan/starch nanocomposite particles was determined as 16–21 nm. The designed novel Pd@chitosan/starch nanocomposite showed superior catalytic behaviour for the synthesis of biphenyl compounds via Suzuki–Miyaura cross-coupling reactions using the microwave irradiation technique which is an alternative source of energy for organic synthesis. Production of biphenyls was carried out under solvent-free conditions and in very short reaction times. Moreover, the prepared palladium nanocomposite showed good reusability in Suzuki–Miyaura reactions due to its ease of recovery from reaction media. The developed catalyst offered many advantages such as high conversion, TONs and TOFs and tolerance to a broad range of functional groups in Suzuki reactions.

ORCID

Talat Baran <http://orcid.org/0000-0003-0206-3841>

Nuray Yilmaz Baran <http://orcid.org/0000-0001-9725-3458>

REFERENCES

- [1] E. Sin, S.-S. Yi, Y.-S. Lee, *J. Mol. Catal. A* **2010**, *315*, 99.
- [2] S.-S. Yi, D.-H. Lee, E. Sin, Y.-S. Lee, *Tetrahedron Lett.* **2007**, *48*, 6771.
- [3] a) S. E. Leonhardt, A. Stolle, B. Ondruschka, G. Cravotto, C. De Leo, K. D. Jandt, T. F. Keller, *Appl. Catal. A* **2010**, *379*, 30; b) T. Baran, *J. Colloid Interface Sci.* **2017**, *496*, 446; c) Y. Dong, X. Wu, X. Chen, Y. Wei, *Carbohydr. Polym.* **2017**, *160*, 106; d) S. Rostamnia, T. Rahmani, *Appl. Organometal. Chem.* **2015**, *29*, 471; e) S. Rostamnia, X. Liu, D. Zheng, *J. Colloid Interface Sci.* **2014**, *432*, 86.
- [4] F. Heidari, M. Hekmati, H. Veisi, *J. Colloid Interface Sci.* **2017**, *501*, 175.
- [5] a) X. Wu, L. Tan, D. Chen, X. Meng, F. Tang, *Chem. Commun.* **2014**, *50*, 539; b) P. Mondal, N. Salam, A. Mondal, K. Ghosh, K. Tuhina, S. M. Islam, *J. Colloid Interface Sci.* **2015**, *459*, 97; c) S. Rostamnia, K. Lamei, F. Pourhassan, *RSC Adv.* **2014**, *4*, 59626; d) S. Rostamnia, B. Zeynizadeh, E. Doustkhah, A. Baghban, K. O. Aghbash, *Catal. Commun.* **2015**, *68*, 77.
- [6] a) A. Baghban, M. Heidarizadeh, E. Doustkhah, S. Rostamnia, P. F. Rezaei, *Int. J. Biol. Macromol.* **2017**, *103*, 1194; b) E. Doustkhah, S. Rostamnia, B. Gholipour, B. Zeynizadeh, A. Baghban, R. Luque, *Mol. Catal.* **2017**, *434*, 7.
- [7] a) P. Zhang, C. Shao, Z. Zhang, M. Zhang, J. Mu, Z. Guo, Y. Liu, *Nanoscale* **2011**, *3*, 3357; b) G.-P. Kim, M. Lee, Y. J. Lee, S. Bae, H. D. Song, I. K. Song, J. Yi, *Electrochim. Acta* **2016**, *193*, 137; c) Z. Zhang, Y. Jiang, M. Chi, Z. Yang, G. Nie, X. Lu, C. Wang, *Appl. Surf. Sci.* **2016**, *363*, 578.
- [8] a) A. Khazaei, M. Khazaei, S. Rahmati, *J. Mol. Catal. A* **2015**, *398*, 241; b) A. Khazaei, S. Rahmati, Z. Hekmatian, S. Saeednia, *J. Mol. Catal. A* **2013**, *372*, 160.
- [9] K. Martina, M. Manzoli, E. C. Gaudino, G. Cravotto, *Catalysts* **2017**, *7*, 98.
- [10] A. Pourjavadi, A. Motamedi, Z. Marvdashti, S. H. Hosseini, *Catal. Commun.* **2017**, *97*, 27.
- [11] P. Das, W. Linert, *Coord. Chem. Rev.* **2016**, *311*, 1.
- [12] a) G. N. Babu, S. Pal, *Tetrahedron Lett.* **2017**, *58*, 1000; b) S. Rostamnia, H. Xin, *Appl. Organometal. Chem.* **2013**, *27*, 348; c) S. Rostamnia, H. Alamgholiloo, X. Liu, *J. Colloid Interface Sci.* **2016**, *469*, 310; d) E. Doustkhah, S. Rostamnia, H. G. Hossieni, R. Luque, *Chem. Select* **2017**, *2*, 329; e) S. Rostamnia, E. Doustkhah, B. Zeynizadeh, *Micropor. Mesopor. Mater.* **2016**, *222*, 87; f) S. Rostamnia, T. Rahmani, H. Xin, *J. Ind. Eng. Chem.* **2015**, *32*, 218.
- [13] B. C. Makhubela, A. Jardine, G. S. Smith, *Appl. Catal. A* **2011**, *393*, 231.
- [14] P. Karthikeyan, A. Vanitha, P. Radhika, K. Suresh, A. Sugumaran, *Tetrahedron Lett.* **2013**, *54*, 7193.
- [15] T. Baran, A. Menteş, *Int. J. Biol. Macromol.* **2015**, *79*, 542.

- [16] Y. Guo, J. Qian, A. Iqbal, L. Zhang, W. Liu, W. Qin, *Int. J. Hydrogen Energy* **2017**, *42*, 15167.
- [17] a) M. Maryami, M. Nasrollahzadeh, E. Mehdipour, S. M. Sajadi, *Sep. Purif. Technol.* **2017**, *184*, 298; b) A. Omidvar, B. Jaleh, M. Nasrollahzadeh, *J. Colloid Interface Sci.* **2017**, *496*, 44.
- [18] A. F. Littke, C. Dai, G. C. Fu, *J. Am. Chem. Soc.* **2000**, *122*, 4020.
- [19] A. Naghipour, A. Fakhri, *Catal. Commun.* **2016**, *73*, 39.
- [20] P. Cotugno, M. Casiello, A. Nacci, P. Mastrorilli, M. M. Dell'Anna, A. Monopoli, *J. Organometal. Chem.* **2014**, *752*, 1.
- [21] N. Jamwal, R. K. Sodhi, P. Gupta, S. Paul, *Int. J. Biol. Macromol.* **2011**, *49*, 930.
- [22] S. Liu, Q. Zhou, H. Jiang, *Chinese J. Chem.* **2010**, *28*, 589.

SUPPORTING INFORMATION

Additional Supporting Information may be found online in the supporting information tab for this article.

How to cite this article: Baran T, Yılmaz Baran N, Menteş A. Sustainable chitosan/starch composite material for stabilization of palladium nanoparticles: Synthesis, characterization and investigation of catalytic behaviour of Pd@chitosan/starch nanocomposite in Suzuki-Miyaura reaction. *Appl Organometal Chem.* 2017; e4075. <https://doi.org/10.1002/aoc.4075>